

Martin N. Yongbi, PhD
Francesco Fera, MD
Yihong Yang, PhD
Joseph A. Frank, MD
Jeff H. Duyn, PhD

Index terms:

Brain, diffusion, 10.121413, 10.12144
Brain, MR, 10.121413, 10.12144
Brain, perfusion, 10.121413
Magnetic resonance (MR), functional imaging, 10.121413, 10.12144
Magnetic resonance (MR), perfusion study, 10.121413

Published online before print
10.1148/radiol.2222001697
Radiology 2002; 222:569–575

Abbreviations:

ASL = arterial spin labeling
CBF = cerebral blood flow
PW = perfusion weighted
ROI = region of interest
SNR = signal-to-noise ratio

¹ From the Laboratory of Functional and Molecular Imaging, Clinical Center (M.N.Y., Y.Y., J.H.D.), and Laboratory of Diagnostic Radiological Research (F.F.), National Institutes of Health, Bethesda, Md; Department of Psychiatry, Functional Neuro-Imaging Laboratory, Cornell University Medical College, New York, NY (J.A.F.); and Institute of Experimental Medicine and Biotechnology, National Research Council, Cosenza, Italy (F.F.). Received October 23, 2000; revision requested December 6; final revision received May 30, 2001; accepted June 20, 2001. Y.Y. supported by the Whittaker Foundation. **Address correspondence** to J.H.D., NMR Center, Building 10, Room BID109, National Institutes of Health, 9000 Rockville Pike, Bethesda, Md 20892.

© RSNA, 2001

Author contributions:

Guarantor of integrity of entire study, M.N.Y.; study concepts, all authors; study design, M.N.Y., J.A.F., J.H.D.; literature research, M.N.Y.; clinical studies, M.N.Y., F.F., J.A.F.; data acquisition, M.N.Y., F.F.; data analysis/interpretation, M.N.Y., Y.Y., F.F., J.A.F., J.H.D.; statistical analysis, M.N.Y., F.F.; manuscript preparation, M.N.Y., F.F., J.H.D.; manuscript definition of intellectual content, M.N.Y., Y.Y., J.A.F., J.H.D.; manuscript editing, revision/review, and final version approval, all authors.

Pulsed Arterial Spin Labeling: Comparison of Multisection Baseline and Functional MR Imaging Perfusion Signal at 1.5 and 3.0 T: Initial Results in Six Subjects¹

Flow-alternating inversion-recovery magnetic resonance imaging was performed at 3.0 T to measure cerebral perfusion during rest and motor activation in six healthy adult volunteers. Results were compared with those at 1.5 T. The mean signal-to-noise ratio for both gray matter and white matter perfusion measured with and without vascular suppression at 3.0 T was significantly ($P < .01$) higher ($n = 6$) than that at 1.5 T. Brain perfusion activation maps collected during a motor task showed a substantially larger number of activated pixels (>80%) at 3.0 T, with activation in the supplementary motor area in the 3.0-T data that was not present on 1.5-T perfusion maps.

Perfusion is a fundamental physiologic process that is highly sensitive to normal tissue function as well as a broad range of pathologic conditions. The potential of magnetic resonance (MR) imaging in the noninvasive measurement of tissue perfusion has been shown in studies of several pathologic conditions, such as stroke (1), dementia (2,3), and epilepsy (4). Techniques for perfusion measurement with MR imaging include monitoring of a bolus of gadolinium-based contrast agent (5,6) and arterial spin labeling (ASL) (7–13). Although techniques based on monitoring of an intravenously administered bolus of contrast agent with

dynamic serial imaging are known to provide better signal-to-noise ratio (SNR), the techniques have a number of drawbacks, including possible adverse patient reaction to the contrast agent and cost. ASL techniques, on the other hand, are entirely noninvasive, but they provide lower SNR. With ASL, arterial water protons that flow into an organ are magnetically labeled and used as an endogenous tracer. The exchange between the labeled arterial blood water and the unlabeled water in tissue leads to a change in tissue magnetization that can be detected at MR imaging.

There are two ASL approaches: continuous and pulsed labeling. In continuous labeling (7,10), tagging is achieved by means of continuous inversion of inflowing arterial water in blood by using a long (~3-second) adiabatic radio-frequency pulse. Pulsed labeling (8,9,11–13), on the other hand, involves use of a relatively short (~10-msec) hyperbolic secant inversion (14) or a frequency-offset-corrected inversion (15) radio frequency for more efficient inversion of the arterial water (16). Although these techniques have become popular for experiments with functional MR imaging (17,18), they are still not used routinely in clinical examinations, primarily because of their characteristic low SNR. This problem is further compounded by additional loss in perfusion signal through T1 as the labeled arterial water protons migrate from the tagging zone to the imaging section. Since the T1 decay rate decreases at higher magnetic field strengths (>3.0 T), the associated perfusion loss is sub-

stantially lower owing to the longer T1 of blood (17).

Despite the apparent advantages of high-field-strength systems, the bulk of ASL studies performed to date have been performed at 1.5 T, with a limited number (reported in abstract form [18]) performed at high field strength. The latter may be due in part to the limited number of whole-body high-field-strength MR imaging systems. Given the expected improvement in perfusion SNR at high field strengths and the progressive increase in the number of 3.0-T MR imagers, there is a need to evaluate the performance of ASL perfusion techniques at higher field strengths, particularly in light of the recent approval of 3.0-T magnets for clinical use by the U.S. Food and Drug Administration.

The goals of this study were to (a) evaluate the feasibility and performance of pulsed ASL techniques for perfusion measurements at 3.0 T and (b) measure the perfusion SNR for gray matter and white matter with and without vascular suppression at 3.0 T and compare with the same data at 1.5 T by means of *t* test analysis. Additionally, the perfusion activation area after a simple motor task was measured at both field strengths, and the activation area was assessed and compared by using standard methods based on functional MR imaging. For this study, we used software and hardware from the same manufacturer.

Materials and Methods

Summary of Perfusion (flow-alternating inversion-recovery) Method

For perfusion measurements in healthy control cerebrum, a modified flow-alternating inversion-recovery sequence (16) was used that incorporates an inversion pulse of the frequency-offset-corrected inversion design (15) for optimal inversion. Although the mode of operation of the flow-alternating inversion-recovery technique has been described elsewhere (8,9), we provide a brief summary as background information.

Perfusion-weighted (PW) MR images are acquired with the flow-alternating inversion-recovery technique by performing two experiments: In the first experiment, a selective inversion radio-frequency pulse (section-selective frequency-offset-corrected inversion in this study) is applied to (ideally) selectively invert only the spins in the imaging volume. As shown in Figure 1, this inversion radio frequency is fol-

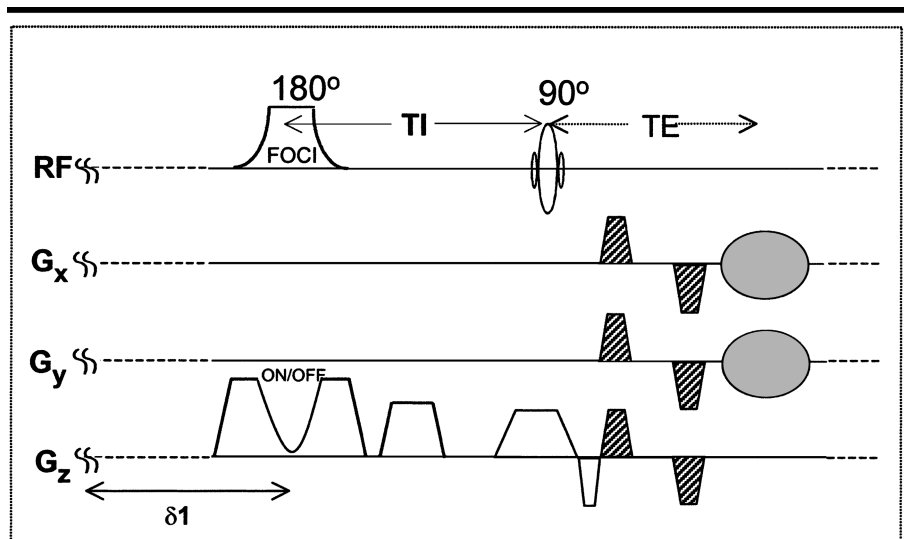


Figure 1. Schematic depicts the flow-alternating inversion-recovery perfusion sequence: a frequency-offset-corrected inversion pulse (*FOCI*) is followed by a delay (*TI*) to allow transit of blood spins to the imaging plane. Signal readout is accomplished with a fast spiral scheme. Gradients (G_x , G_y , G_z) within the inversion time are used to spoil unwanted transverse magnetization created by the inversion pulse. The frequency-offset-corrected inversion gradient waveform is switched on for selective inversion and off for nonselective (control) flow-alternating inversion-recovery acquisitions. The bipolar gradient lobes (diagonal lines) within the echo time (*TE*) denote the gradients are applied to minimize signal contributions from the vascular bed. *RF* = radio frequency, $\delta 1$ = recovery delay.

lowed by a delay period (inversion time) during which uninverted fresh blood flows into the imaging section, and some exchange with the tissue protons occurs. This exchange increases the bulk apparent relaxation rate in the voxel, which results in an image with signal intensity that is flow weighted. In the second experiment (interleaved with the first), image acquisition is performed with identical timings but with the inversion radio frequency rendered nonselective by switching the frequency-offset-corrected inversion gradient off. In this manner, all incoming blood spins into the section are inverted so that any subsequent exchange with tissue spins does not alter the relaxation rate; hence, a non-flow-weighted image is acquired. The PW images are obtained by subtracting the non-flow-weighted image from the flow-weighted image.

Clinical Studies

Clinical studies were performed with 1.5- and 3.0-T MR imaging systems (Lx; GE Medical Systems, Milwaukee, Wis) that included identical hardware and software platforms. A quadrature head coil was used for radio-frequency transmission and reception. The studies were performed as part of a protocol approved by the Intramural Review Board at the National Institutes of Health. Informed

consent was obtained from all volunteers before they participated in the study.

Multisection brain perfusion images (10 transverse 5-mm-thick sections) were acquired in six healthy volunteers (three men and three women; age range, 23–30 years; mean age, 26 years). In each subject, 1.5- or 3.0-T MR imaging was performed on a different day. The age range was limited to between 23 and 30 years to minimize age dependency on the perfusion signal. Since the total imaging volume was 50 mm thick (ie, 10 sections \times 5 mm), an inversion width of the same size should (ideally) be used in the selective inversion radio-frequency pulse to minimize the transit time of blood to the imaging volume. Unfortunately, use of an inversion width equal to the width of the imaging slab causes interaction between the pulses, which results in contamination from static tissue. On the basis of findings in previous calibration experiments (16), we used a selective inversion width of 80 mm. Bipolar crusher gradients with an amplitude of 15 mT/m (2-msec duration and separation) were applied (Fig 1) to selectively eliminate contributions from large vessels (10,13). In some experiments, the crusher-gradient pulses were switched off to allow the acquisition of PW images with vascular signal intensity.

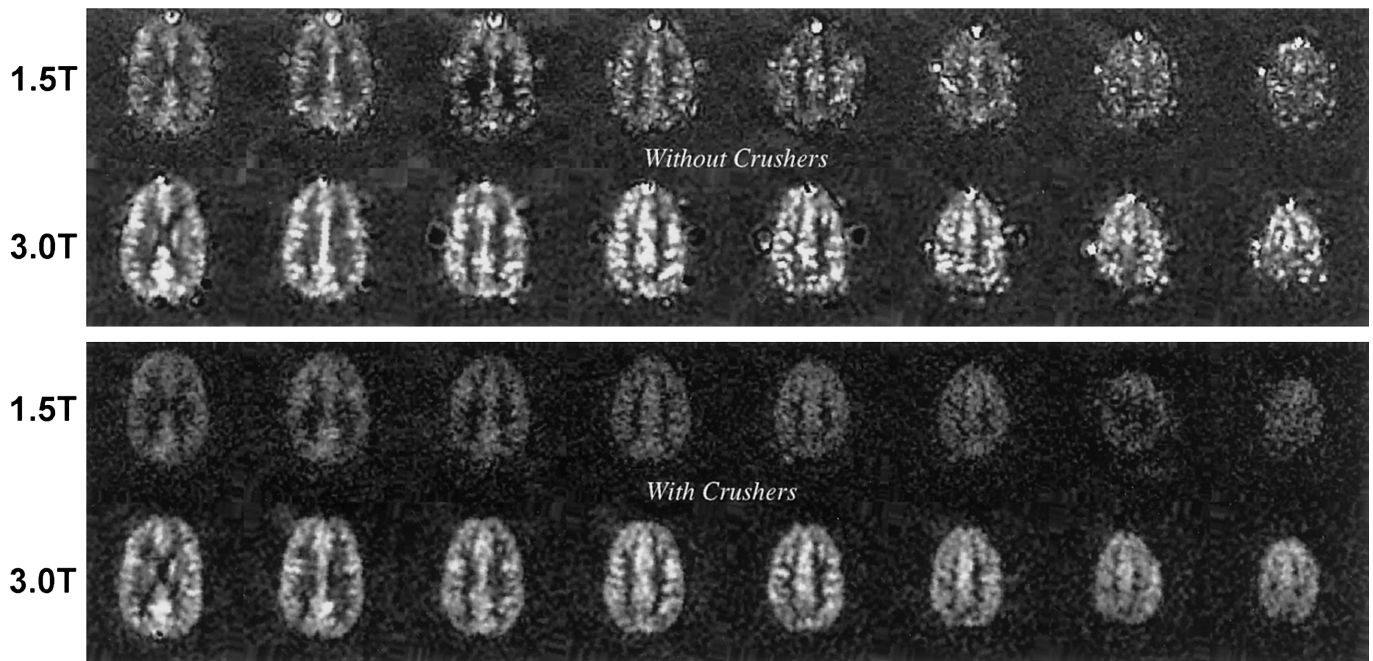


Figure 2. Top: Multisection PW images acquired in human brain without vascular signal suppression at 1.5 and 3.0 T are displayed with the same window and level settings. Localized areas of high signal intensity (artifacts) represent intravascular signal contributions (eg, from the sinus and other peripheral vessels). Bottom: Corresponding PW images in the same subject were acquired with vascular signal suppression. The bulk of the vascular artifacts have been eliminated by using the crusher gradients.

For absolute regional cerebral blood flow (CBF) quantification, PW images were acquired with a series of 11 inversion time values that ranged from 0.5 to 3.3 seconds. These data permitted the estimation of transit times, on the basis of subsequent signal versus inversion time curves for PW images, which were then used to quantify CBF, as previously described (13). Other imaging parameters included recovery delay, 2.5 seconds; echo time, 17 msec; field of view, 240 mm; 40 flow-weighted and non-flow-weighted raw images to calculate the PW images. To estimate the perfusion SNR, 120 flow-weighted and non-flow-weighted raw images were used to calculate the PW images. Inversion time for the latter measurement was set to 1.8 seconds with crusher gradients and 1.3 seconds without crusher gradients, because these values are known to provide optimal perfusion sensitivity under the two given crusher-gradient conditions (13,17). The spiral readout involved use of trapezoidal gradients to achieve minimal T2* weighting and to minimize the effects of blood oxygenation level dependence. The duration of this pulse was 22 msec, which is substantially shorter than that implemented in most current echo-planar sequences.

Given the widespread use of ASL techniques for functional MR imaging inves-

tigations, we also conducted experiments to compare the perfusion-related activation signals at both field strengths by using a simple motor task. Forty perfusion images were collected in 4 minutes (ie, 6 seconds for each flow-alternating inversion-recovery image) during which subjects ($n = 4$) alternated between rest (off state) and finger tapping (on state). There were four off and four on states, which each lasted 30 seconds. The finger-tapping frequency was paced at 1 Hz by using a computer-controlled digit that was regularly projected on a visible screen to indicate when the subject should finger tap with the thumb of the subject's dominant hand (right in all cases). The other parameters (recovery delay, 1,575 msec; echo time, 7 msec; inversion time, 1,200 msec; field of view, 24 cm; matrix, 64×64 ; five sections acquired) combined to yield a PW image every 6 seconds. In each examination, the preceding experiment was repeated five times in the same subject to test for reproducibility.

Data Analyses

Both baseline perfusion and functional MR imaging data were analyzed offline with a workstation (SunSparc; Sun Microsystems, Palo Alto, Calif) by using functional MR imaging software (MEDX; Sensor Systems, Sterling, Va) and programs

written in-house (Interactive Data Language [IDL]; Research Systems, Boulder, Colo). To obtain perfusion data, the non-selective raw images were subtracted from the corresponding selective flow-weighted images. The resultant PW images were averaged to provide a PW image with a relatively high SNR for each inversion time. For SNR estimates, regions of interest (ROIs) (12–15 pixels) were manually prescribed in maps of segmented gray matter and white matter by using the functional MR imaging display software. Segmentation of the gray matter and white matter was based on pre-calculated T1 maps by using nonselective inversion-recovery images for each subject. The T1-based ROIs for segmentation of gray matter and white matter were then transferred to the same spatial locations on the flow-alternating inversion-recovery PW images, and their mean signal intensity was calculated.

Noise was computed as the SD in a 12–15-pixel ROI that was free of signal intensity and placed outside the PW images in the upper left corner of the image. Images for which the measured noise was more than 5% of the noise estimated on a reference (signal intensity-free) image acquired with parameters identical to those used to acquire the PW images, but with the radio-frequency pulses switched off, were excluded. In this study, the

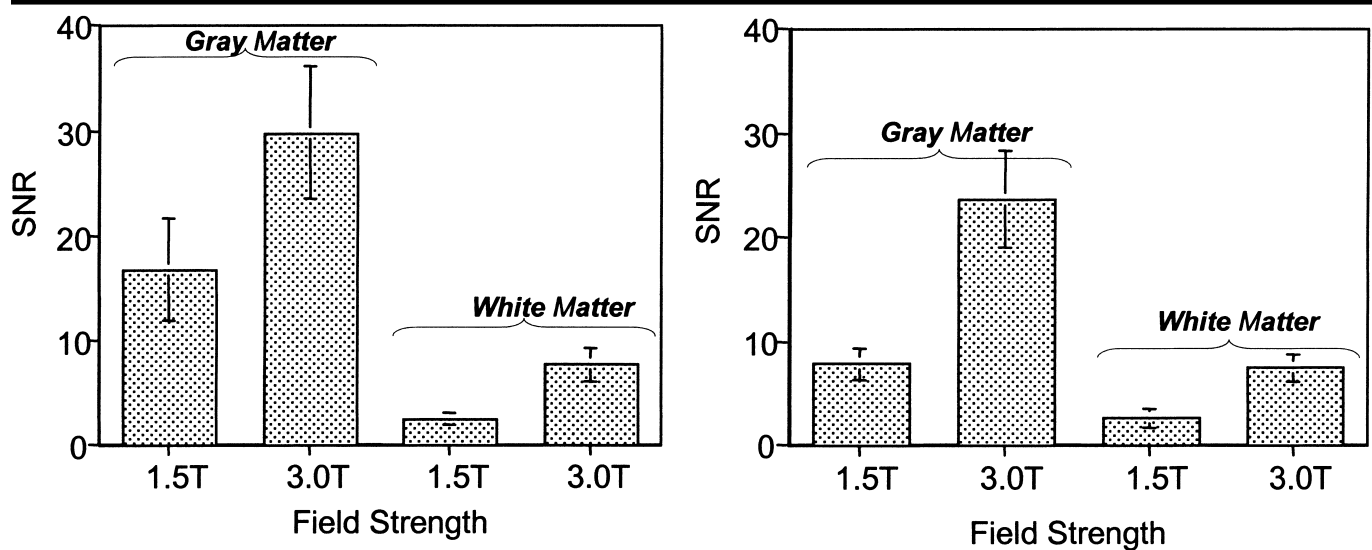


Figure 3. Bar graphs depict perfusion SNR at 1.5 and 3.0 T. Left: Plot for data acquired without vascular signal suppression. Right: Plot for data acquired with vascular signal suppression. The higher perfusion SNR on the left is primarily due to contributions from the unsuppressed flowing spins within the vascular bed. Higher perfusion SNR at 3.0 T is attributed mainly to the increase in T1 of arterial blood, which in turn minimizes the amount of decay of the tag in transit to the imaging volume. Error bars indicate the SD.

number of excluded PW images ranged between zero and three. The mean perfusion SNR with and without vascular suppression was measured for both gray matter and white matter at both field strengths. A *t* test analysis was then performed to assess for significant differences between the mean gray matter perfusion SNR and the mean white matter perfusion SNR across the two magnetic fields. These analyses were conducted separately within each technique (ie, with and without vascular suppression).

To further compare the perfusion performance at both field strengths and to estimate absolute CBF, the normalized perfusion-related signal change was integrated in gray matter and white matter ROIs. The ROI approach provided adequate SNR to allow multiparameter fit of the wash-in and washout curves from which transit times were estimated by using previously described methods (13). All ROI prescriptions in this study were performed by one neuroradiologist (F.F.).

Automated image registration performed with the software sought to minimize the sampling coefficient of variation of ratios of voxel values between the first raw image and each successive raw image. Perfusion activation maps were obtained with a pixel-wise cross correlation of perfusion signal-to-time courses with a boxcar reference function that reflected the activation paradigm. For this study, only pixels with a significant activation ($P < .05$) were included.

Summary of Transit Times and Absolute CBF Measured in Gray Matter and White Matter at 1.5 and 3.0 T

Finding	Subject No.					
	1	2	3	4	5	6
Transit time (msec)						
1.5 T						
Gray matter*	0.66	0.70	0.72	0.70	0.72	0.60
White matter†	0.88	0.79	0.70	0.83	0.81	0.68
3.0 T						
Gray matter‡	0.54	0.62	0.53	0.77	0.65	0.78
White matter§	0.70	0.82	0.72	0.85	0.70	0.78
CBF (mL/100 g/min)						
Gray matter						
1.5 T	71.2	60.0	62.2	62.0	57.0	72.6
3.0 T#	73.0	66.3	59.2	70.8	58.2	63.0
White matter						
1.5 T**	22.7	20.9	26.6	31.3	22.9	20.8
3.0 T††	27.6	22.0	19.7	25.2	26.8	36.6

* Mean \pm SD, 0.68 ± 0.05 .

† 0.78 ± 0.08 .

‡ 0.65 ± 0.11 .

§ 0.76 ± 0.06 .

|| 64.1 ± 6.3 .

65.1 ± 6.1 .

** 24.2 ± 4.1 .

†† 26.3 ± 5.0 .

Results

Figure 2 shows representative PW images acquired at both field strengths without (top) or with (bottom) the application of vascular signal suppression crusher-gradient pulses. Images obtained with both field strengths manifested clean subtraction and excellent gray matter and white matter contrast, which are

characteristic of spin-tagging perfusion images (10–13). However, improved performance at 3.0 T in terms of better SNR was observed, and a quantitative analysis was performed. Typical signal intensity components from large vessels (vascular artifacts), which were observed as bright spots on the perfusion images obtained with crusher gradients, were effectively

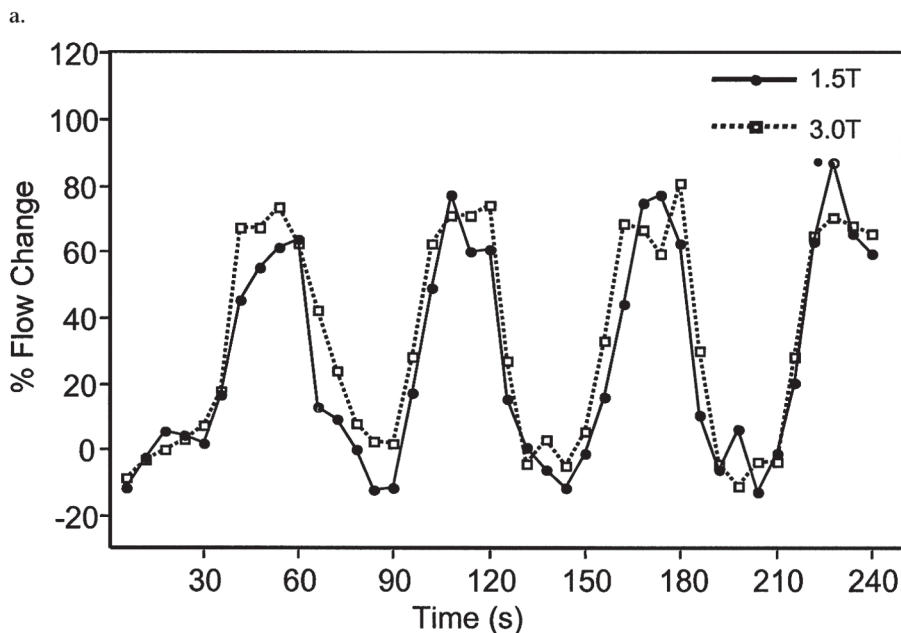
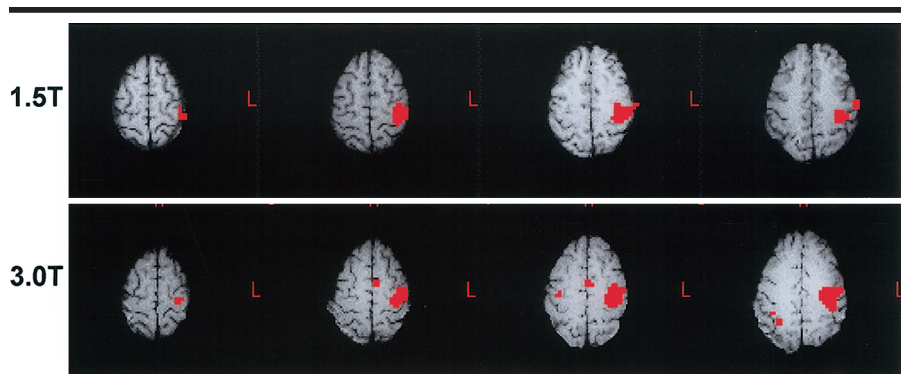


Figure 4. (a) Perfusion activation maps at 1.5 and 3.0 T obtained in a motor activation study during finger tapping overlaid on T1-weighted images. Activated pixels in the supplementary and primary motor regions are depicted in red. (b) Graph depicts mean perfusion signal change ($n = 4$) from the primary motor area in the images in a at both field strengths. Activation in supplementary and contralateral motor areas was observed at only 3.0 T mainly because of higher perfusion SNR.

eliminated at both field strengths by using a crusher-gradient intensity of approximately 7 sec/mm^2 .

The mean gray matter perfusion SNR (23.7 ± 9.3 [SD]) acquired with vascular suppression at 3.0 T was found to be significantly higher ($P < .01$) than the corresponding gray matter perfusion SNR (8.3 ± 2.2) obtained at 1.5 T. For the white matter images acquired with vascular suppression, the mean perfusion SNR (6.8 ± 2.3) was also significantly higher ($P < .01$) than the corresponding mean value (2.7 ± 1.5) at 1.5 T. These results are depicted in Figure 3. The mean perfusion SNR obtained without vascular suppression also manifested a similar trend in both the mean gray matter (30.0 ± 6.1) and white matter (8.4 ± 2.2)

at 3.0 T, which indicates significantly higher ($P < .01$) values than the corresponding mean gray matter (17.1 ± 5.2) and mean white matter (2.7 ± 1.3) values at 1.5 T. These results are also shown in Figure 3.

The average perfusion signals in gray matter or white matter were measured and normalized to the equilibrium magnetization. For the central section, the change (qualitative and quantitative) in signal with vascular signal suppression manifested the typical wash-in and wash-out characteristic curve (13). At both field strengths, the perfusion signal progressively increased as inversion time increased and reached a broad plateau centered at an inversion time of around 1.8 seconds. The perfusion signal then de-

clined as a function of inversion time owing to the competing mechanisms of the inflow of fresh spins and T1 effects with increasing inversion time (17). However, the perfusion signal was consistently higher at 3.0 T throughout the entire inversion time range.

For comparison with results in other groups, the perfusion signal was normalized by dividing it by the equilibrium magnetization (ie, the normalized perfusion-related signal change), since this ratio is independent of the total number of images. Gray matter normalized perfusion-related signal change was a mean $0.708\% \pm 0.109$ at 3.0 T and $0.598\% \pm 0.079$ at 1.5 T. The corresponding white matter normalized perfusion-related signal change at 3.0 T was $0.184\% \pm 0.063$ of equilibrium magnetization and $0.120\% \pm 0.044$ at 1.5 T.

Mean CBF values for the gray matter and white matter ROIs at 3.0 T in the healthy volunteers were $65.1 \text{ mL}/100 \text{ g}/\text{min} \pm 6.1$ and $26.3 \text{ mL}/100 \text{ g}/\text{min} \pm 5.9$, respectively, with a mean gray matter to white matter CBF ratio of 2.5. Similar results were obtained at 1.5 T. They are summarized in the Table because they have already been reported (10,13).

The activation maps obtained from one subject at both field strengths (overlaid on high-spatial-resolution T1-weighted images) are shown in Figure 4a. Despite similarities in the location of motor activation, the 3.0-T images showed a substantially greater extent of activation. The mean number of activated voxels for data from four subjects were $128 \text{ voxels} \pm 34$ at 3.0 T (z score, 6.79 ± 0.45) compared with $70 \text{ voxels} \pm 12$ at 1.5 T (z score, $5.52 \text{ voxels} \pm 0.32$).

The increased number of activated voxels at 3.0 T can be primarily ascribed to the better perfusion SNR at 3.0 T and, to a lesser extent, to reduced transit time losses owing to the longer T1 of blood. More important, perfusion-related activation was consistently observed in the ipsilateral primary and contralateral supplementary motor area on 3.0-T images. On the contrary, no activation of these regions appeared on the 1.5-T images for the same statistical threshold used in the analysis. An overlay plot of the perfusion-related time courses obtained at both field strengths in identical ROIs in the primary motor cortex is shown in Figure 4b. The signal plots represent the mean of five measurements in the same subject, and they show a perfusion increase during activation of around 70% in both cases. The similarity in activation-induced blood flow change is ex-

pected since this increase is independent of field strength.

Discussion

To date, the bulk of spin-labeling studies designed to measure tissue perfusion have been performed at 1.5 T (8–13). Higher magnetic field strengths provide higher SNR. Even though T2 losses and susceptibility effects increase with field strength, findings in this study clearly show that high-quality pulsed arterial spin-tagging perfusion images in human brain are readily obtained at 3.0 T with excellent suppression of static background tissue signal. Absolute CBF and measured values for change in signal divided by the signal were in excellent agreement with previously published experimental data (for 1.5 T) (10,13) and theoretically predicted values for both field strengths (17).

Compared with findings on perfusion images acquired at 1.5 T, the improvement in perfusion signal intensity afforded by the increased field strength is readily apparent from our results. The mean increase in perfusion SNR in gray matter at 3.0 T was substantially greater than that observed for white matter. This discrepancy may be due to the differences in transit time between gray matter and white matter, which was shown in a recent study (19–21) to be approximately 0.5 second longer in white matter than in gray matter. Given the exponential loss of perfusion signal with transit time (10,13), the perfusion signal increase in white matter that results from the increased field strength is likely to be severely offset by transit time losses. In our implementation, we attempted to minimize this problem by using the highly selective frequency-offset-corrected inversion pulse (15,16) in place of the conventional hyperbolic secant pulse (14).

SNR values reported for both field strengths depend primarily on the measurement parameters used and the hardware resources that are available. For example, the perfusion SNR will be different for different imaging section thickness, as will other measurement parameters, such as echo time, repetition time, or both. Furthermore, the use of multiple receive (phased-array) coils will likely enhance the perfusion signal. Because T2* losses are lower at 1.5 T, it may be possible to use a longer spiral readout, which would result in the use of a smaller receiver bandwidth and consequently reduce receiver fold-back

noise into the MR images. While this approach may be suitable for single-section ASL studies, it is not appropriate for multisection investigations because it can cause big intersection inversion time differences and quantitative problems. Additionally, the shorter readout duration is desired especially at higher field strengths (3.0 T in this study) to minimize the effects of both T2* and blood oxygenation level dependence on the PW images.

In most functional MR imaging investigations, the simultaneous measurement of blood oxygenation level dependence and perfusion-based activation can provide complementary information. Therefore, a more complete investigation would incorporate measurements of blood oxygenation level dependence obtained with functional MR imaging. However, the measurements of blood oxygenation level dependence were precluded primarily because they have been performed previously (22,23).

In performing the perfusion comparison, we attempted to control for possible variations between the two imagers that may bias the results. For example, we controlled for experimental parameters, manufacturer hardware, and processing software. Owing to the possibility of spatial mismatch in section positioning between the two field strengths, normalization of the data to a standardized space may have been necessary. The latter requirement was minimized by using standard in-house equipment at both field strengths to secure the volunteer's head in the same spatial position within the standard head coil. Further consistency in spatial localization was ensured by using high-spatial-resolution T1-weighted images as a guide. Additionally, the latter task was performed in all subjects by the same observer (F.F.).

Findings in our study demonstrate that high-quality ASL perfusion images can be acquired at 3.0 T with significant improvement in SNR over measurements performed at 1.5 T. ASL approaches to MR imaging of CBF offer the potential for completely noninvasive quantitative imaging of an important physiologic and diagnostic quantity. For clinical perfusion studies, however, approaches that involve use of dynamic contrast agents still remain the main choice primarily because of better SNR performance. Inadequate SNR continues to be the main drawback in the clinical application of ASL-based techniques. For example, despite the increased sensitivity observed in the current 3.0-T study, absolute quanti-

fication of perfusion was possible only with measurements performed over relatively large ROIs from data acquired during 45 minutes. However, the situation is completely different for functional MR imaging applications for which the improved perfusion sensitivity at 3.0 T clearly results in more precise mapping of brain function. Future studies are needed that focus on further improvements in ASL perfusion sensitivity, particularly in conjunction with the use of multiple receiver coils.

References

1. Detre JA, Alsop DC, Vives LR, Maccotta L, Teener JW, Raps EC. Noninvasive MRI evaluation of cerebral blood flow in cerebrovascular disease. *Neurology* 1998; 50:633–641.
2. Frackowiak RSJ, Pozzilli C, Legg NJ, et al. Regional cerebral oxygen supply and utilization in dementia. *Brain* 1981; 104:753–778.
3. Waldemar G. Functional brain imaging with SPECT in normal aging and dementia. *Cerebrovasc Brain Metab Rev* 1995; 7:89–130.
4. Spencer SS. The relative contributions of MRI, SPECT, and PET imaging in epilepsy. *Epilepsia* 1994; 35(suppl):S72–S89.
5. Belliveau JW, Rosen BR, Kantor HL, et al. Functional cerebral imaging by susceptibility contrast. *Magn Reson Med* 1990; 14:538–546.
6. Ostergaard L, Sorenson AG, Kwong KK, Weisskoff RM, Glyndensted C, Rosen BR. High resolution measurement of cerebral blood flow using intravascular tracer bolus passages. II. Experimental comparison and preliminary results. *Magn Reson Med* 1996; 36:726–736.
7. Williams DS, Detre JA, Leigh JS, Koretsky AP. Magnetic resonance imaging of perfusion using spin inversion of arterial water. *Proc Natl Acad Sci U S A* 1992; 89:212–216.
8. Kwong KK, Chesler DA, Weisskoff RM, et al. MR perfusion studies with T1-weighted echo planar imaging. *Magn Reson Med* 1995; 34:878–887.
9. Kim SG. Quantification of relative cerebral blood flow change by flow sensitive alternating inversion recovery (FAIR) technique: application to functional mapping. *Magn Reson Med* 1995; 34:293–301.
10. Ye FQ, Pekar JJ, Jezzard P, Duyn JH, Frank JA, McLaughlin AC. Perfusion imaging of the human brain at 1.5 T using a single-shot EPI spin tagging approach. *Magn Reson Med* 1996; 36:219–224.
11. Tanabe JL, Yongbi M, Branch CA, Hrabe J, Johnson G, Helpert JA. MR perfusion imaging in human brain using the UNFAIR technique. *J Magn Reson Imaging* 1999; 9:761–767.
12. Wong EC, Buxton RB, Frank LR. Quantitative imaging of perfusion using a single subtraction (QUIPSS and QUIPPS II). *Magn Reson Med* 1998; 39:702–708.
13. Yang Y, Frank JA, Hou L, Ye FQ, McLaughlin AC, Duyn JH. Multislice imaging of quantitative cerebral perfusion with pulsed arterial spin labeling. *Magn Reson Med* 1998; 39:825–832.

14. Silver MS, Joseph RI, Hoult DI. Selective spin inversion in nuclear magnetic resonance and coherence optics through an exact solution of the Bloch-Riccati equations. *Phys Rev* 1985; A31:2753-2755.
15. Ordidge RJ, Wylezinska M, Hugg JW, Butterworth E, Franconi F. Frequency offset corrected inversion (FOCI) pulses for use in localized spectroscopy. *Magn Reson Med* 1996; 36:562-566.
16. Yongbi MN, Yang Y, Frank JA, Duyn JH. Multislice perfusion imaging in human brain using the C-FOCI inversion pulse: comparison with hyperbolic secant. *Magn Reson Med* 1999; 42:1098-1105.
17. Kim SG, Tsekos NV, Ashe J. Multi-slice perfusion based functional MRI using the FAIR technique: comparison of CBF and BOLD effects. *NMR Biomed* 1997; 10: 191-196.
18. Kastrup A, Li TQ, Glover GH, Kruger G, Mosley ME. Gender differences in cerebral blood flow and oxygenation response during focal physiologic neural activity. *J Cereb Blood Flow Metab* 1999; 19:1066-1071.
19. Calamante F, Williams SR, van Bruggen N, Kwong KK, Turner R. A model for quantification of perfusion in pulsed labeling techniques. *NMR Biomed* 1996; 8:79-83.
20. Duvvuri U, Roberts DA, Bolinger L, Schnall MD. Quantitative perfusion imaging at 4.0 T (abstr). In: Proceedings of the Sixth Meeting of the International Society for Magnetic Resonance in Medicine. Berkeley, Calif: International Society for Magnetic Resonance in Medicine, 1998; 1201.
21. Ye FQ, Mattay VS, Frank JA, Weinberger DR, McLaughlin AC. Comparison of white and gray matter arterial transit times in spin-tagging experiments (abstr). In: Proceedings of the Seventh Meeting of the International Society for Magnetic Resonance in Medicine. Berkeley, Calif: International Society for Magnetic Resonance in Medicine, 1999; 1847.
22. Bandettini PA, Wong EC, Jesmanowicz A, et al. MRI of human brain activation at 0.5 T, 1.5 T, and 3.0 T: comparison of ΔR_2 and functional contrast to noise ratio (abstr). In: Proceedings of the First Meeting of the Society of Magnetic Resonance. Berkeley, Calif: Society of Magnetic Resonance, 1994; 434.
23. Yang Y, Wen H, Mattay VS, Balaban RS, Frank JA, Duyn JH. Comparison of 3D BOLD functional MRI with spiral acquisition at 1.5 T and 4.0 T. *Neuroimage* 1999; 446-451.